

FIG. 2

Compound	D-Value Pd II	Conformation Minimum Energy (kcal/mole)	Connectivity Index (order 2, standard) D	Dipole Moment (debye) E	Electron Affinity (eV) F
DQ 18	2.86	39.331	11.632	12.744	7.127
DQ 16		39.449	11.985	2.933	6.601
DQ 10	1.75	40.322	12.692	0.01	5.948
DQ 14	2.6	39.924	11.071	25.323	8.122
DQ 17	3.3	50.797	17.289	25.52	7.139
DQ 15	0.42	49.902	17.642	0.025	6.597
DQ 12	1.59	50.899	18.349	0.124	5.946
DQ 13	3.22	50.293	16.728	52.726	8.119
DQ11	0.89	49.694	16.935	0.148	7.867

FIG. 3A

Compound	Dielectric Energy (kcal)/mole) G	Steric Energy (kcal/mole) H	Total Energy (Hartree) I	Heat of Formation (kcal/mole)	HOMO Energy (ev)
DQ 18	7.7	39.331	214.593	258.295	13.703
DQ 16	7.211	39.597	221.775	242.427	13.635
DQ 10	6.602	40.322	236.121	218.102	13.52
DQ 14	8.438	39.924	205.938	291.32	13.855
DQ 17	7.759	50.797	329.153	171.131	12.628
DQ 15	7.301	49.902	336.331	155.69	12.601
DQ 12	6.62	50.899	350.679	131.143	12.552
DQ 13	8.487	50.293	320.496	204.337	12.687
DQ11	8.312	49.694	321.968	190.296	12.661

FIG. 3B

Compound	Ionization Potential (eV) L	Log P M	LUMO (eV) Energy N	Shape Index (basic kappa, order 3) O	Valence Connectivity Index (order 2, standard) Q	Solvent Accessible Surface Area (Å ²) P
DQ 18	13.703	6.409	-7.127	21.031	521.24	11.069
DQ 16	13.635	6.86	-6.601	22.027	539.815	11.423
DQ 10	13.52	7.653	-5.948	23.967	576.054	12.13
DQ 14	13.855	6.179	-8.122	13.04	485.397	10.53
DQ 17	12.628	12.75	-7.139	36.681	813.7	16.726
DQ 15	12.601	13.201	-6.598	37.686	831.853	17.08
DQ 12	12.552	13.993	5.946	39.658	883.721	17.787
DQ 13	12.687	12.52	-8.119	26.747	778.615	16.187
DQ11	12.661	12.697	-7.867	35.716	793.278	16.372

FIG. 3C

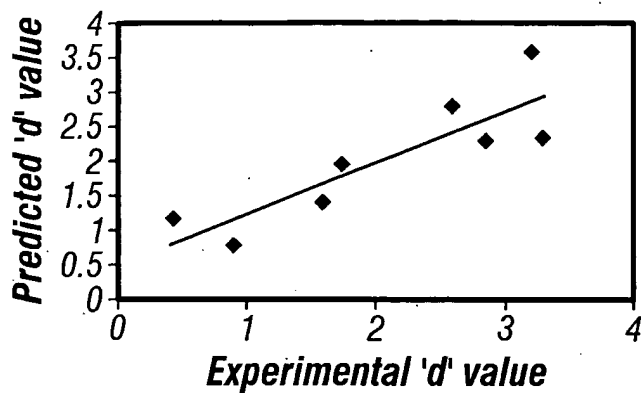


FIG. 4A

Predictive Eq. for Pd II

$$B = 0.0554277 * E + 0.610452 * L - 16.7616 / N - 9.0729$$

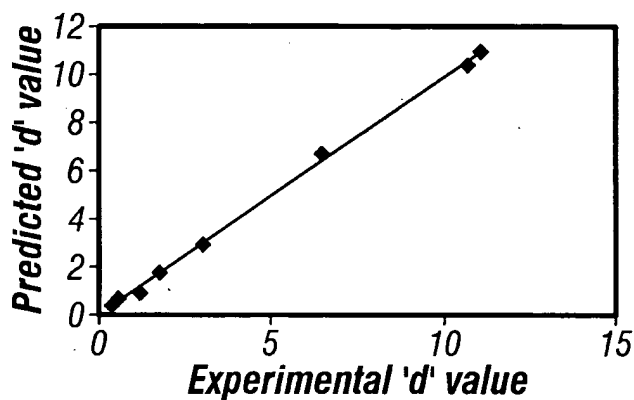


FIG. 4B

Predictive Eq. for Pd IV

$$B = 71.6336 * D + 0.463796 * E + 23.6272 * F + 19.8848 * G - 9.37422 * H + 2.71931 * I + 108.256$$

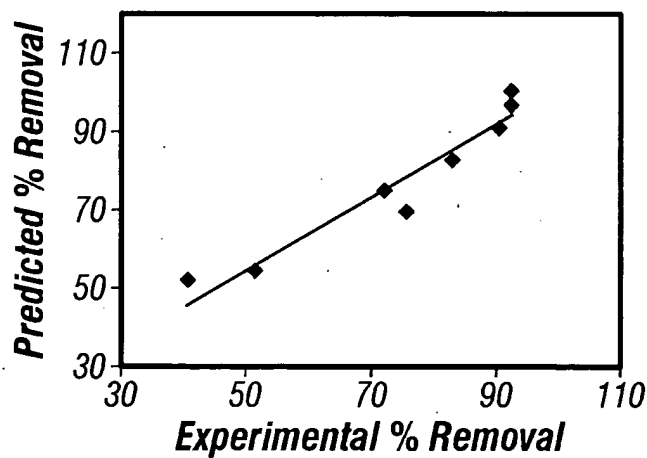
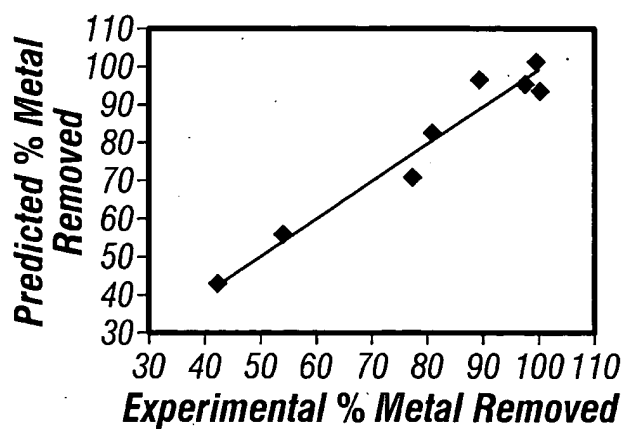


FIG. 4C

Predictive Eq. for Pt II

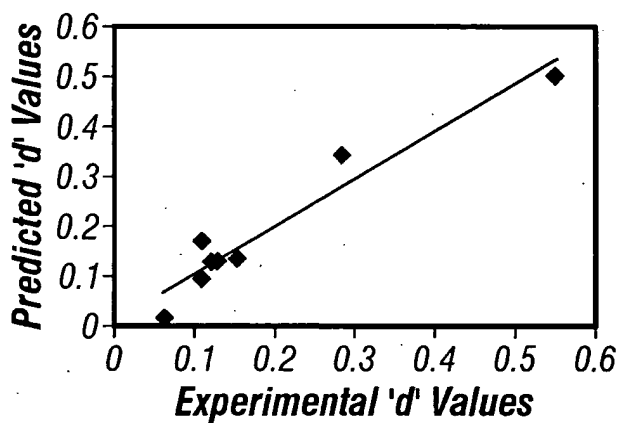
$$B = -276.194 * L - 69.6714 * M - 4.68162 * N - 7.67628 * O + 3.7778 * P - 154.864 * Q + 4211.14$$



Predictive Eq. for Pt IV

$$B = 283.378 * D + 1.4239 \\ 9 * E + 173.825 * F + 212.2 \\ 66 * G + 2.69479 * H + 14 \\ 4354 * I + 167.3$$

FIG. 4D



Predictive Eq. for Rh III

$$B = 0.00584793 * E - \\ 0.90334 * N - 42.1486 / N - \\ 12.3346$$

FIG. 4E

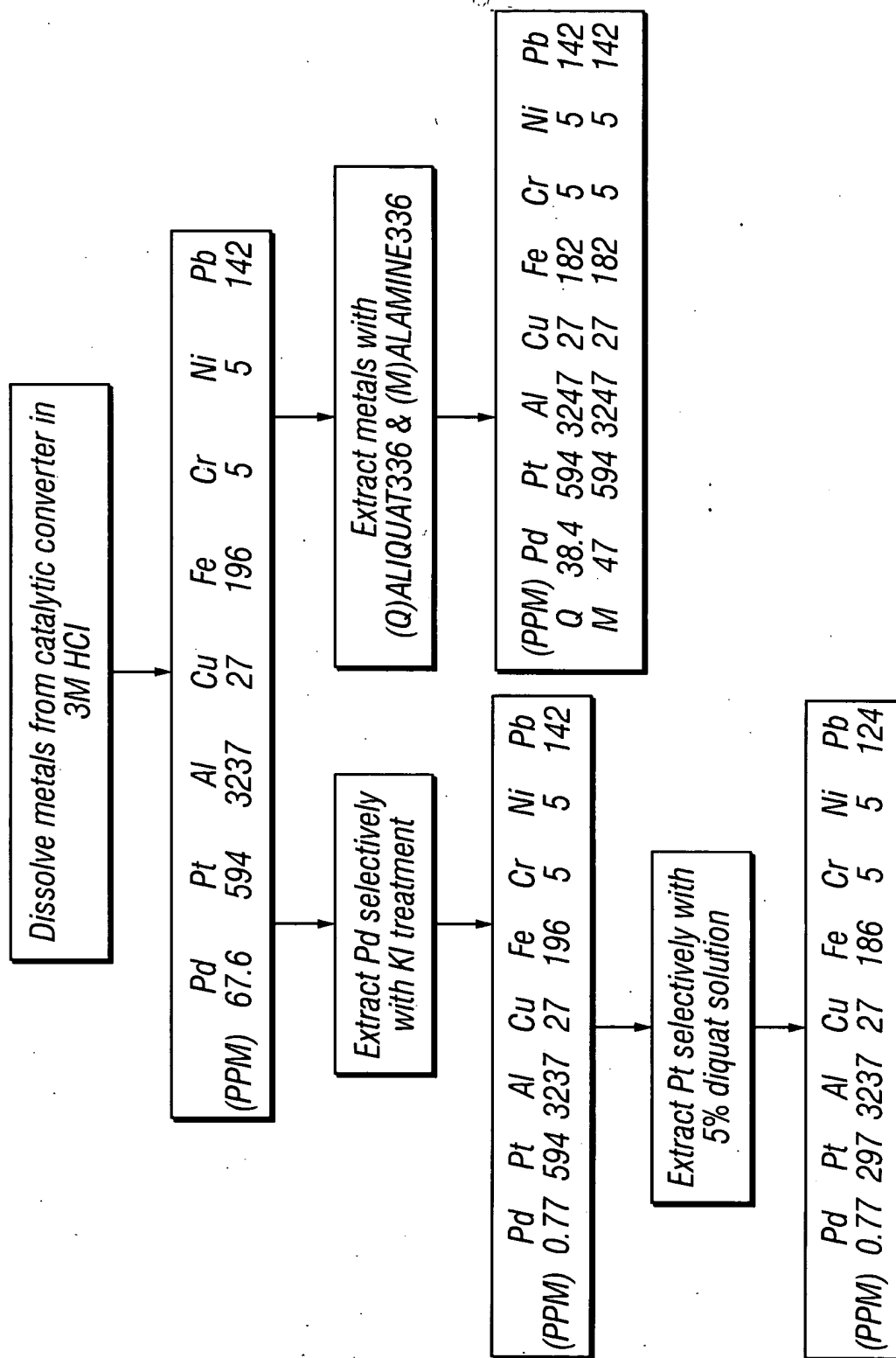


FIG. 5

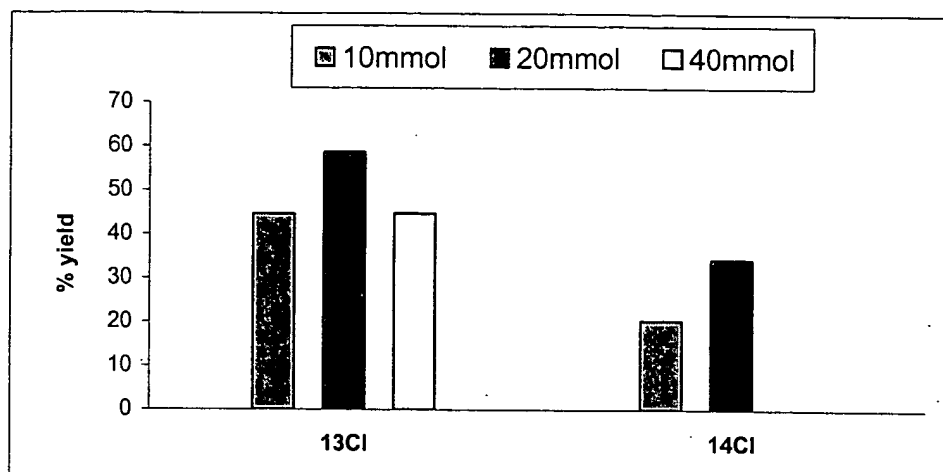


Figure 6. Effect of scale up of synthesis on yields of the reaction

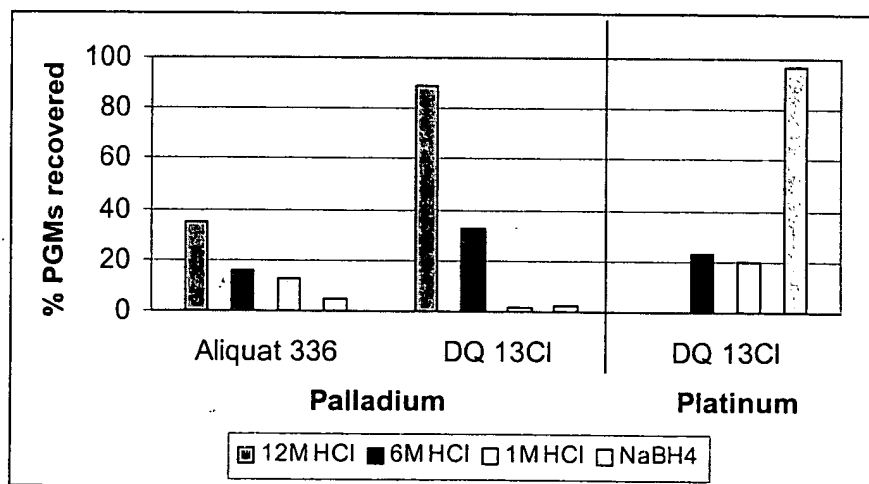


Figure 7. Comparison of % of PGMs recovered during back extraction experiments

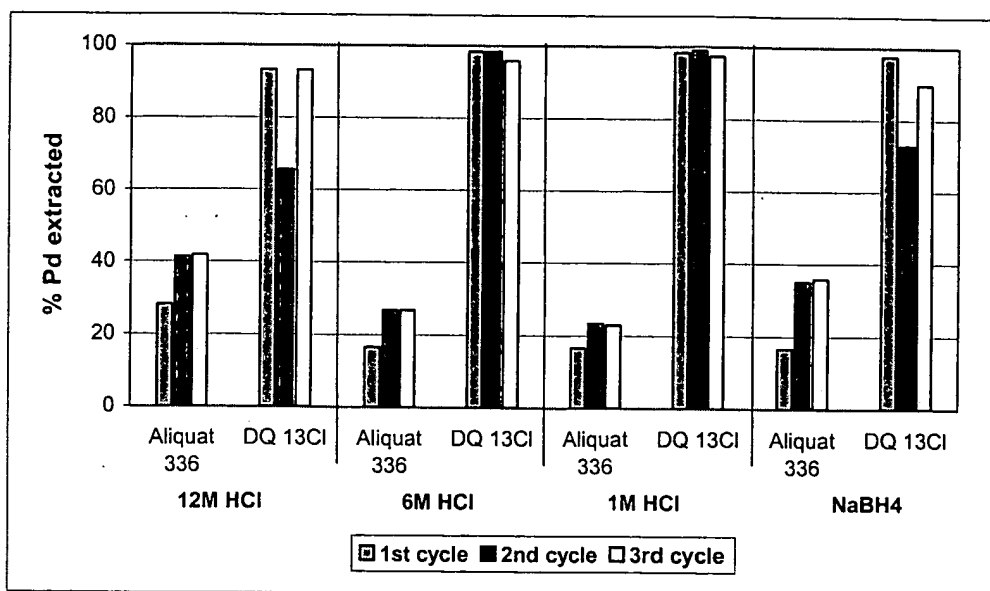


Figure 8. Comparison of efficiency of diquats in multiple extractions

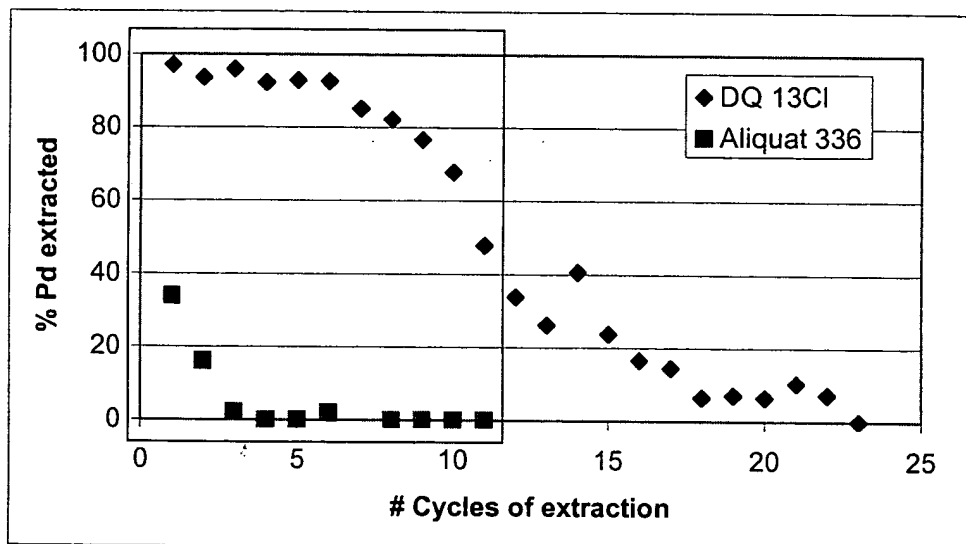


Figure 9. Efficiency of DQ 13Cl in continuous Pd extractions

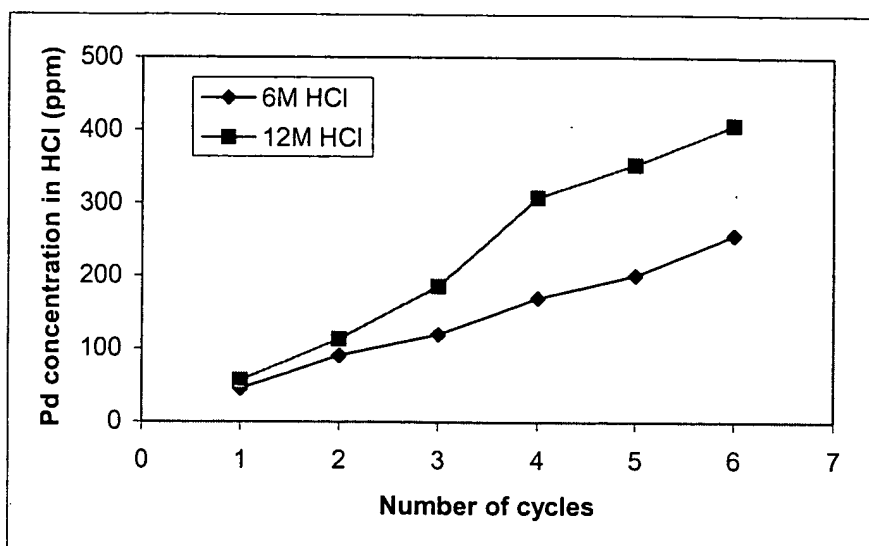


Figure 10. Concentration of Pd back-extracted in HCl

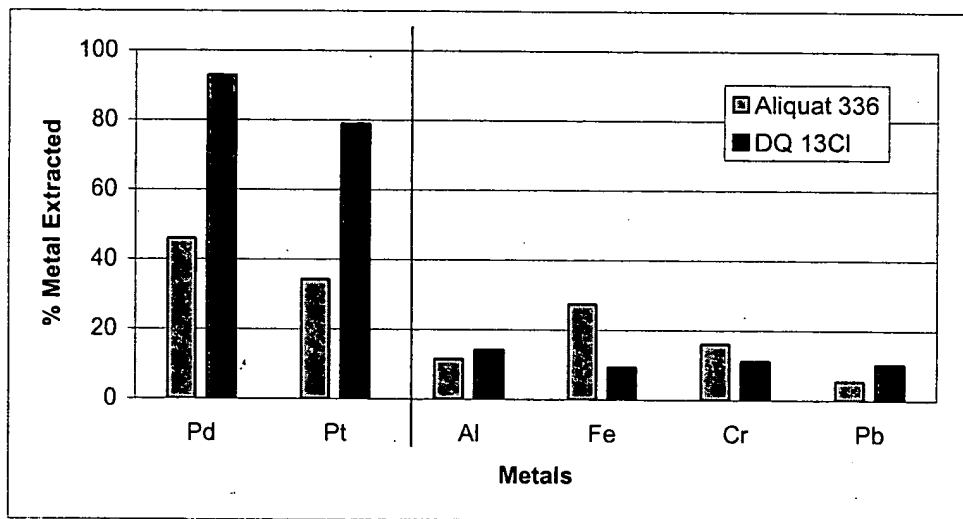


Figure 11. Selectivity of diquats towards extractability of PGMs from base metals

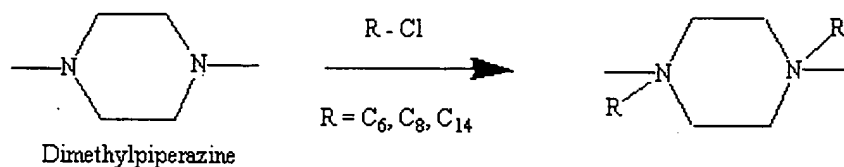


Figure 12. Synthetic scheme for synthesis of new diquaternary amine compounds

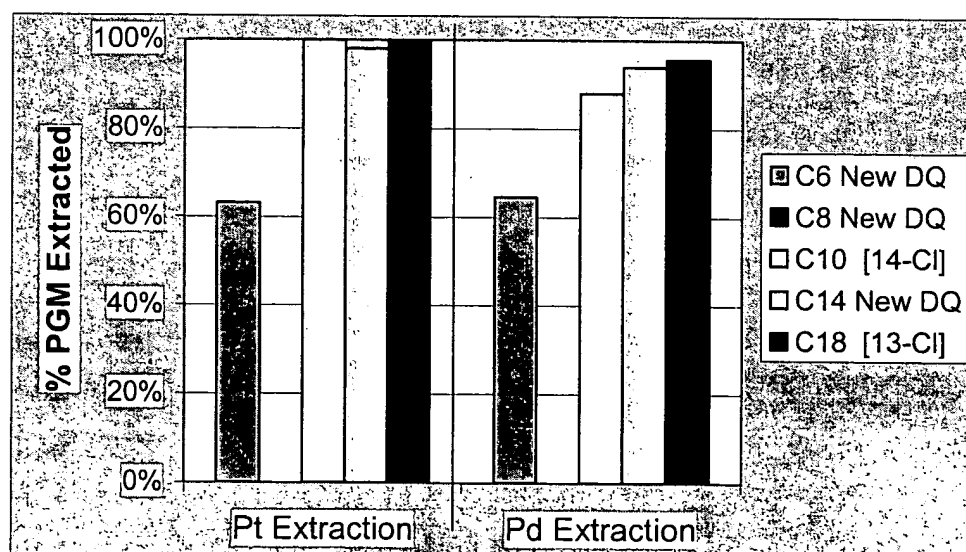


Figure 13. Longer side chain substitution increases PGM extraction efficiency

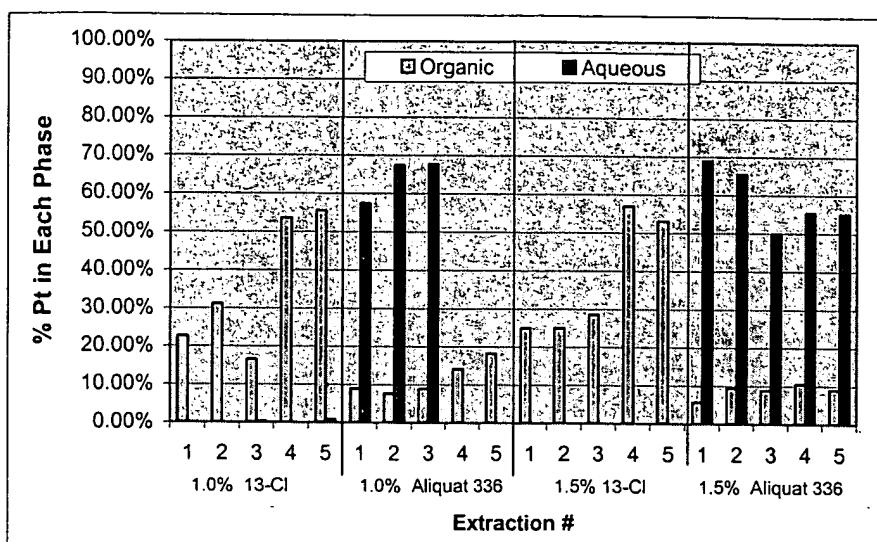


Figure 14. Material Balance Investigation of PGM's

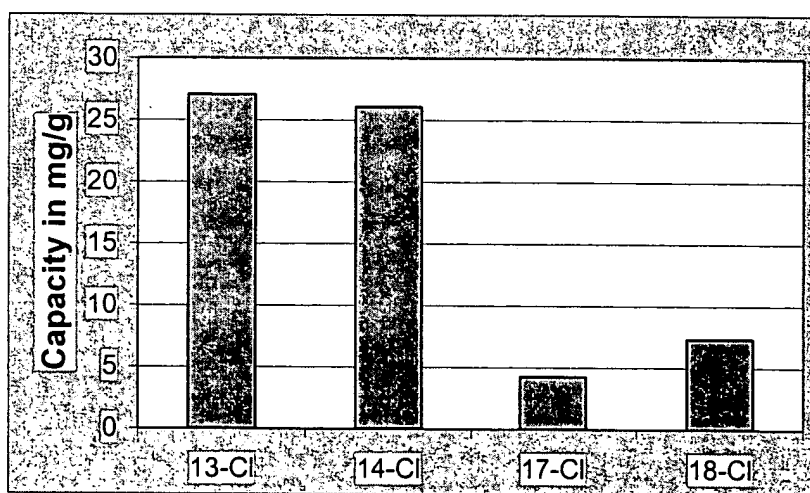


Figure 15. Binding Capacities of different diquats

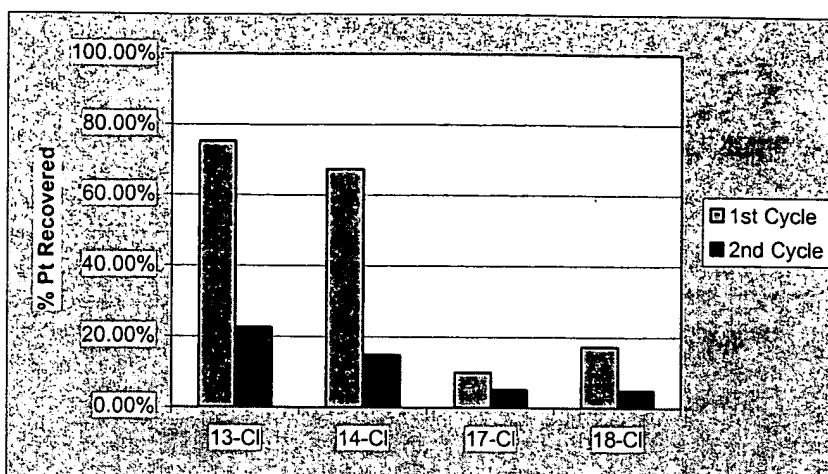


Figure 16. 13-Cl and 14-Cl outperform 17-Cl and 18-Cl and continue to extract a majority of PGMs at low concentrations.

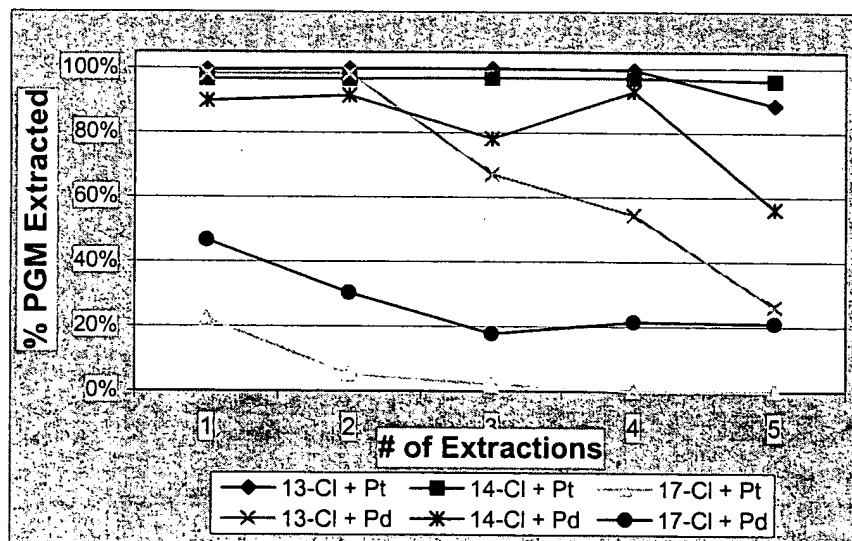


Figure 17. 13-Cl and 14-Cl continue to extract over 90% of PGM's in multiple extractions

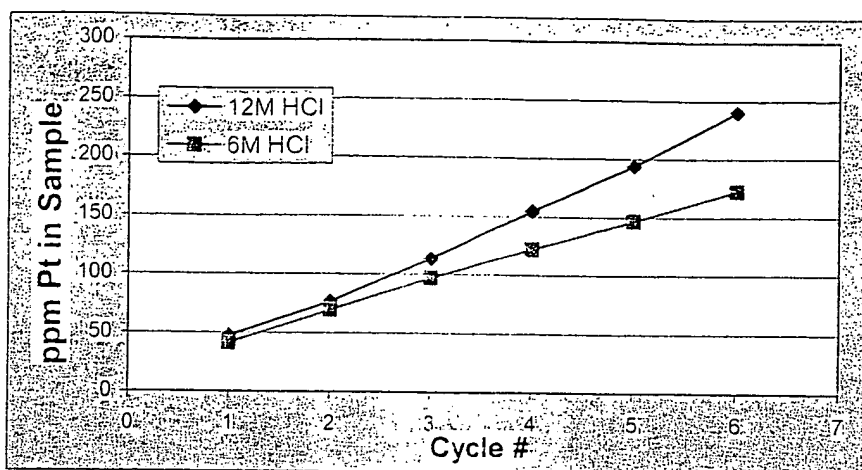
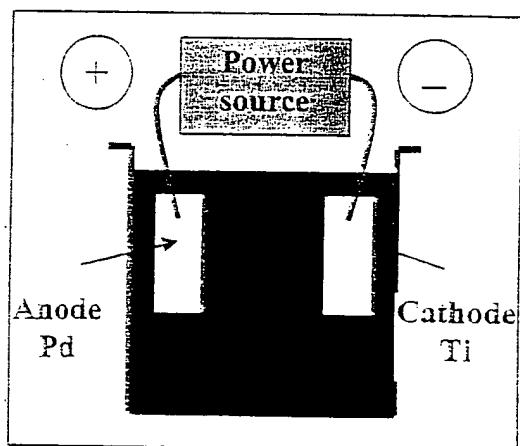


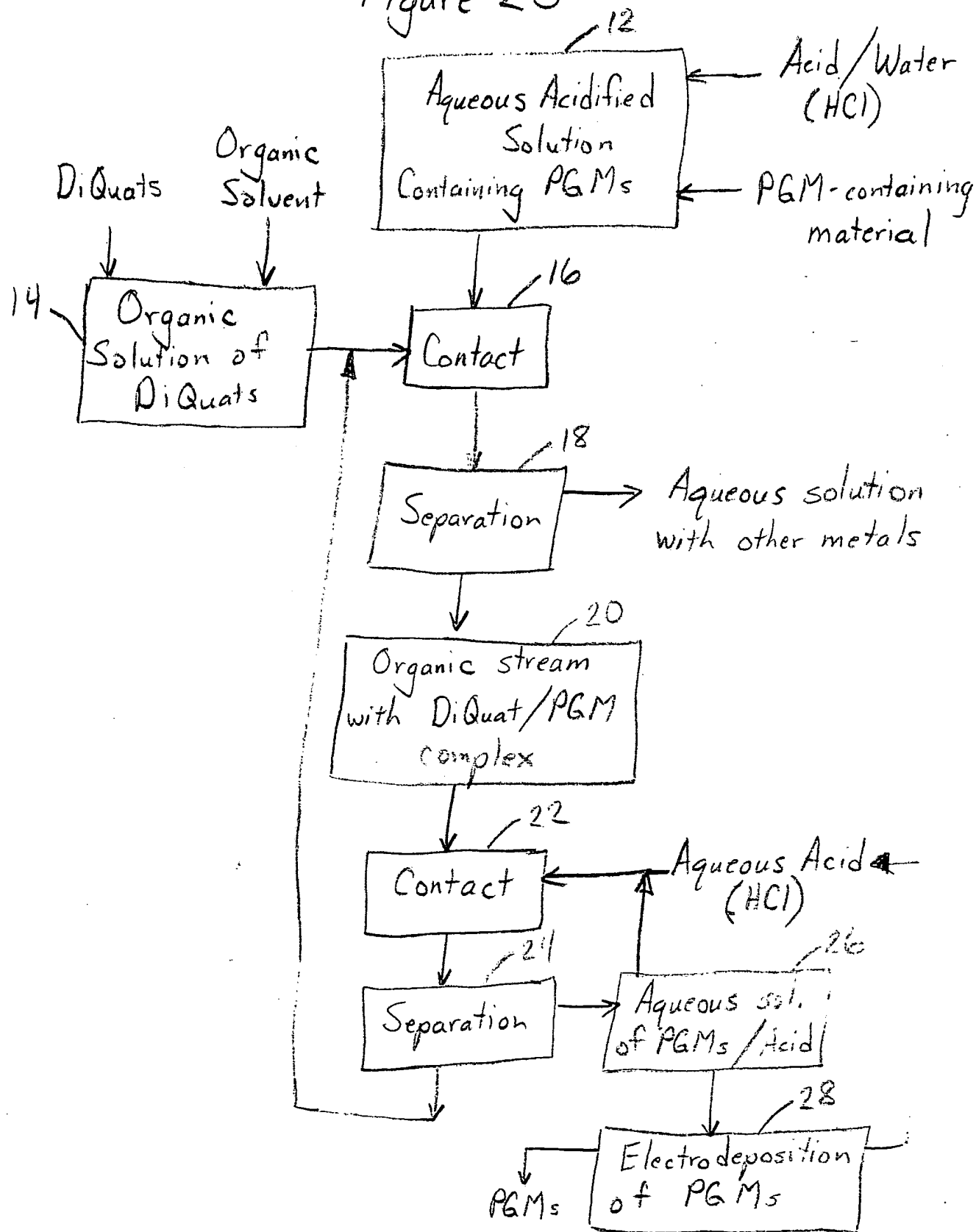
Figure 18. HCl can be reused effectively for multiple back extractions

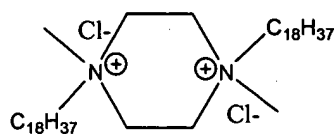
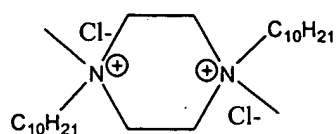
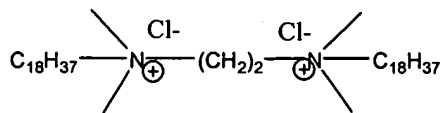
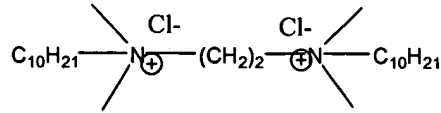
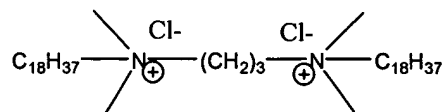
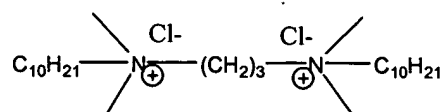
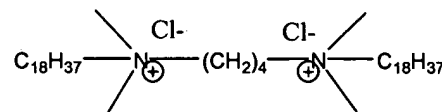
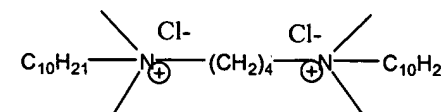
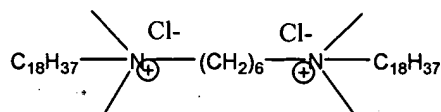
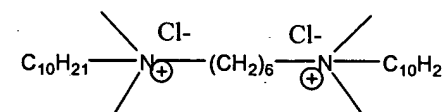
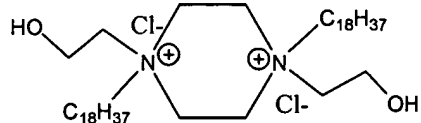
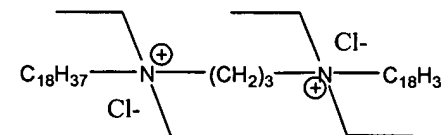
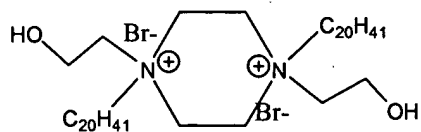
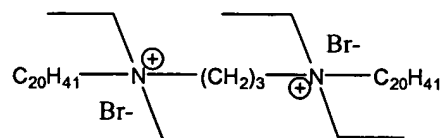
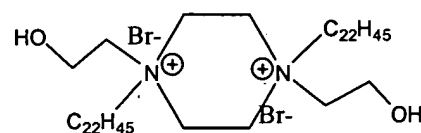
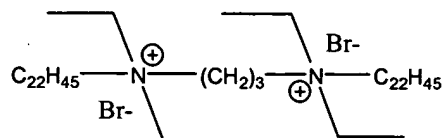


Schematic diagram of electro deposition

Figure 19

Figure 20



**DQ 13-Cl****DQ 14-Cl****DQ 11-Cl****DQ 9-Cl****DQ 17-Cl****DQ 18-Cl****DQ 15-Cl****DQ 16-Cl****DQ 12-Cl****DQ 10-Cl****DQ C18-HyPip****DQ C18-Et4Me3****DQ C20Br-HyPip****DQ C20Br-Et4Me3****DQ C22Br-HyPip****DQ C22Br-Et4Me3****Figure 21. Structures of the Synthesized Diquats.**

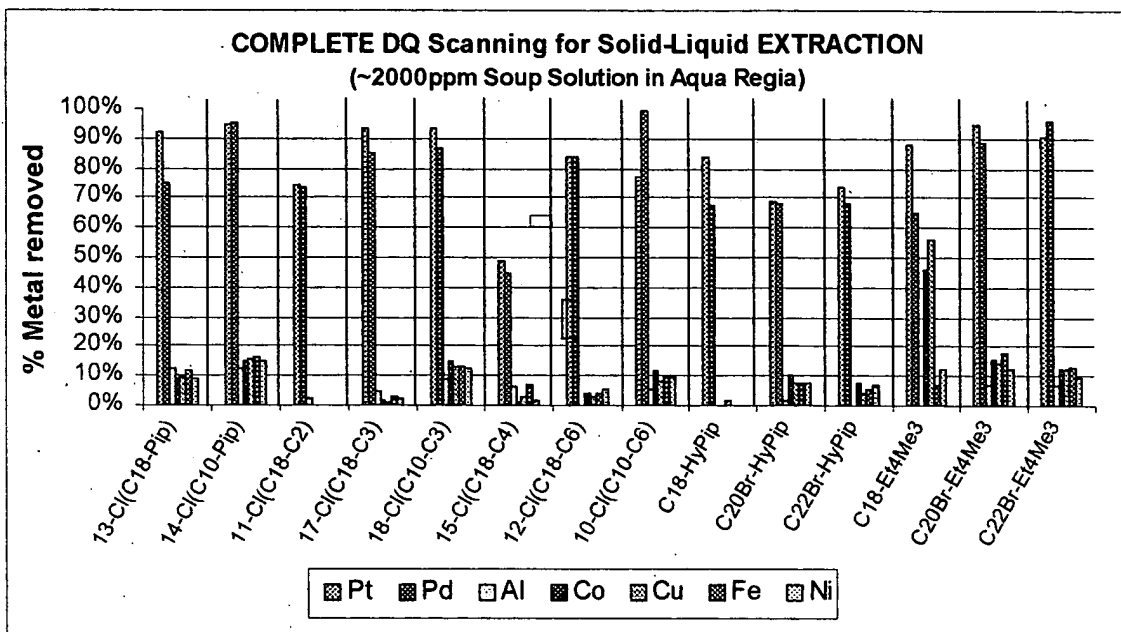


Figure 22. Selective PGM Extraction by Diquats using Solid-Liquid Extraction Process

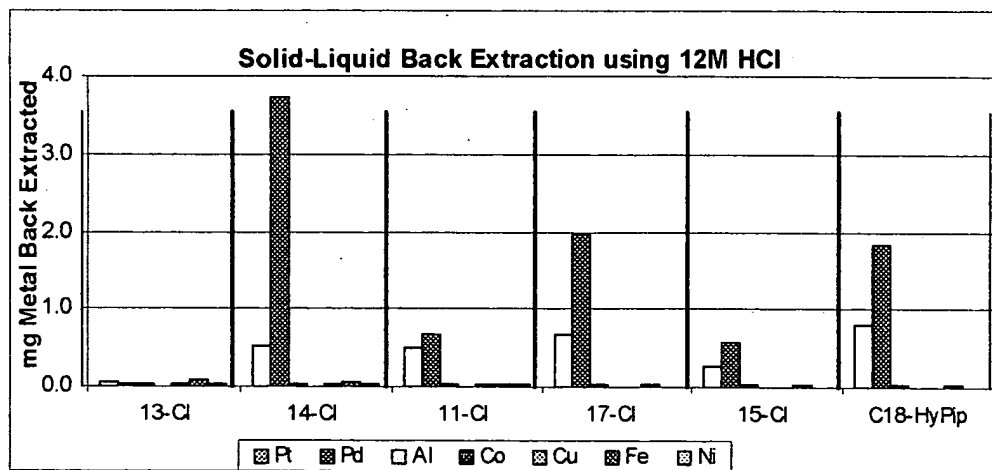


Figure 23. 12M HCl can be used for Back-Extraction of PGMs

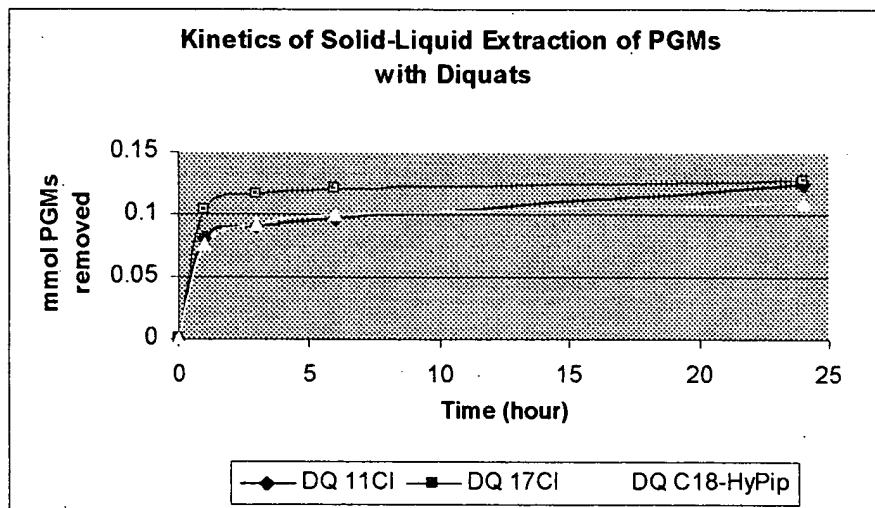


Figure 24. The PGMs removal efficiency becomes steady in an hour.

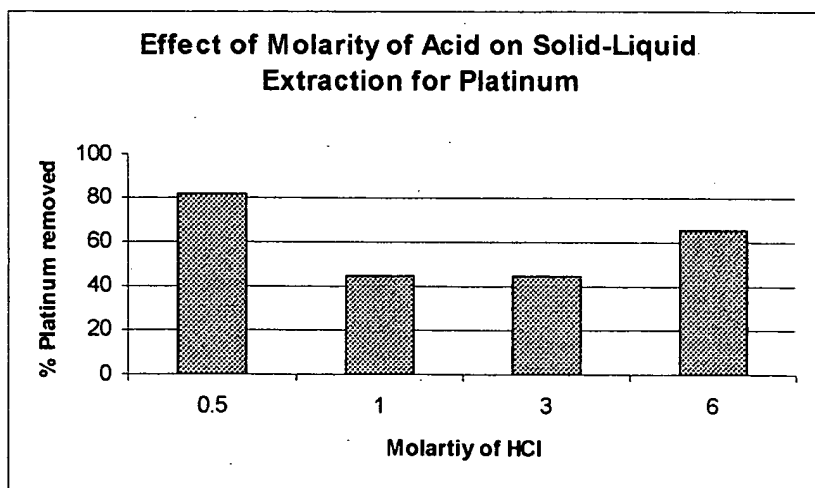


Figure 25. The effect of molarity on solid-liquid extraction is in investigation.

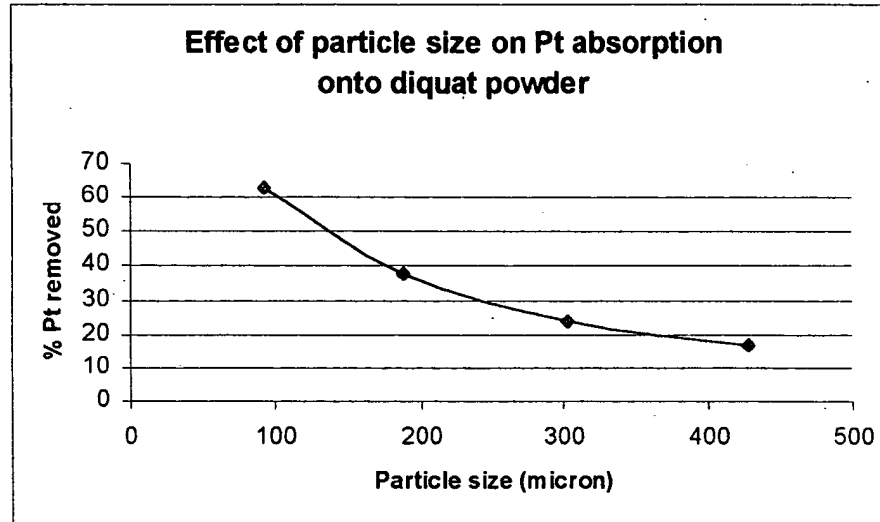


Figure 26. Since smaller particles have more relative surface area, fine particles removed more platinum. Customers can choose a particle size compromising the backpressure and PGM removal efficiency in their systems.

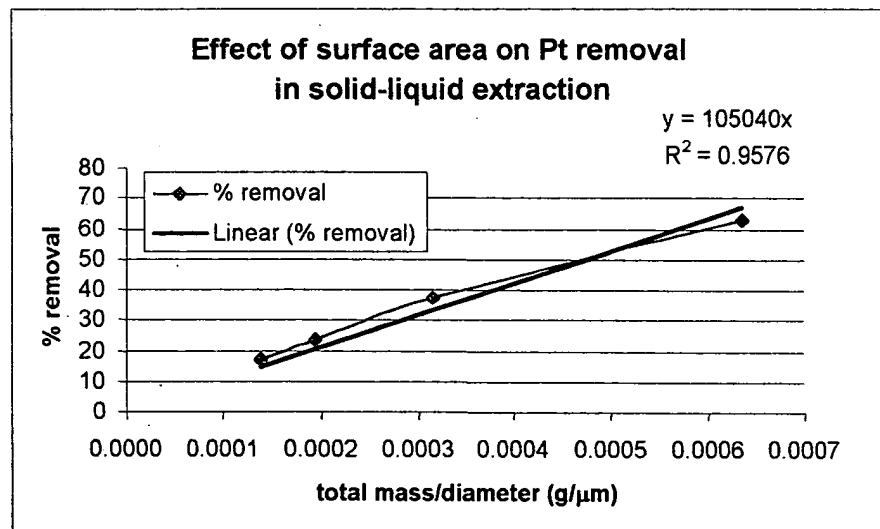


Figure 27. Total surface area=total mass/diameter of a particle. There is a linear relationship between the total surface area and platinum removal efficiency.

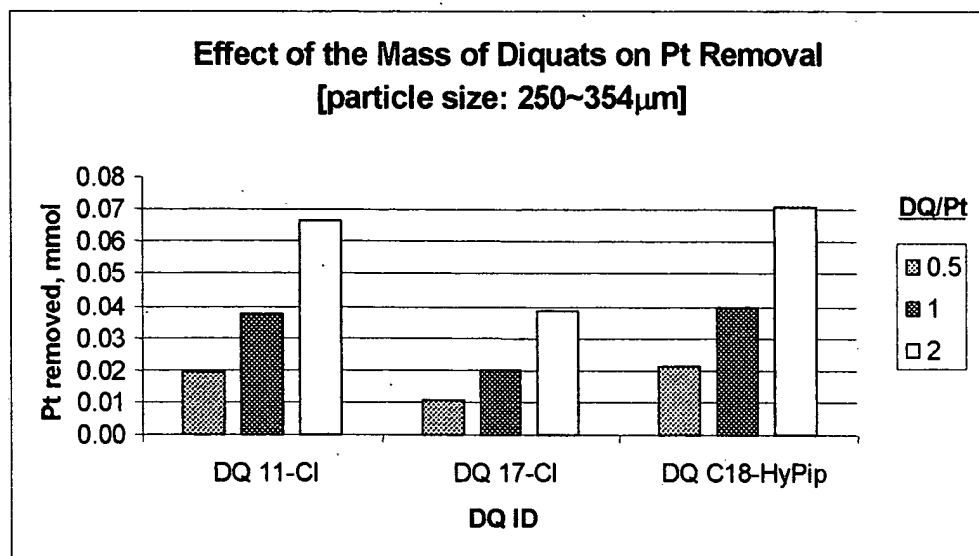


Figure 28. The efficiency of solid-liquid extraction decreased by adding more absorbents in case of DQ 11-Cl and DQ 17-Cl. The efficiency was reasonably increasing with DQ C18-HyPip according to the ratio between the diquat and platinum.

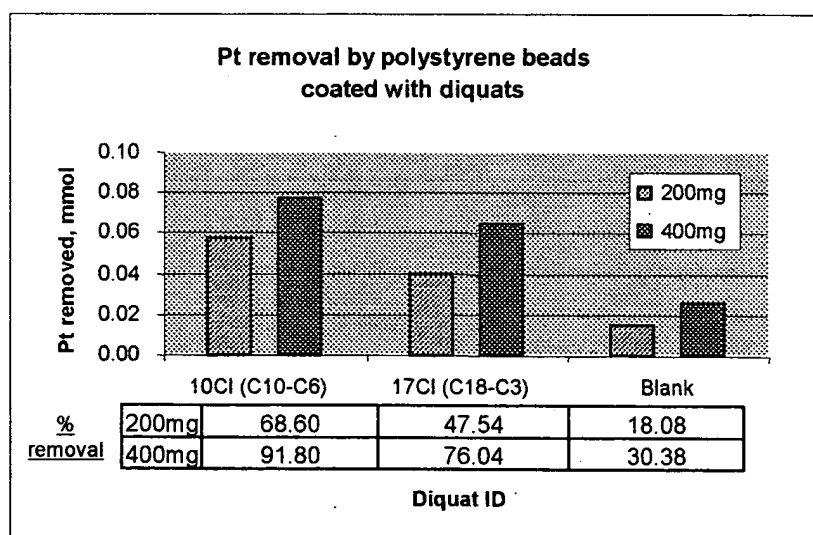


Figure 29. Diquat-coated polystyrene beads successfully removed platinum ions from the aqueous solution.